Global Drought Watch from Space

Felix N. Kogan
National Oceanic and Atmospheric Administration/National Environmental Satellite Data and Information Service, Camp Springs, Maryland

ABSTRACT

Drought is the most damaging environmental phenomenon. During 1967–91, droughts affected 50% of the 2.8 billion people who suffered from weather-related disasters. Since droughts cover large areas, it is difficult to monitor them using conventional systems. In recent years the National Oceanic and Atmospheric Administration has designed a new Advanced Very High Resolution Radiometer- (AVHRR) based Vegetation Condition Index (VCI) and Temperature Condition Index (TCI), which have been useful in detecting and monitoring large area, drought-related vegetation stress. The VCI was derived from the Normalized Difference Vegetation Index (NDVI), which is the ratio of the difference between AVHRR-measured near-infrared and visible reflectance to their sum. The TCI was derived from the 10.3–11.3-μm AVHRR-measured radiances, converted to brightness temperature (BT). Algorithms were developed to reduce the noise and to adjust NDVI and BT for land surface nonhomogeneity. The VCI and TCI are used to determine the water- and temperature-related vegetation stress occuring during drought. This paper provides the principles of these indices, describes data processing, and gives examples of VCI–TCI applications in different ecological environments of the world. The results presented here are the first attempt to use both NDVI and thermal channels on a large area with very diversified ecological resources. The application of VCI and TCI are illustrated and validated by in situ measurements. These indices were also used for assessment of drought impact on regional agricultural production in South America, Africa, Asia, North America, and Europe. For this purpose, the average VCI–TCI values for a given region and for each week of the growing season were calculated and compared with yields of agricultural crops. The results showed a very strong correlation between these indices and yield, particularly during the critical periods of crop growth.

1. Introduction

In the late 1980s, the United Nations called for global efforts in minimizing the harm from natural disasters. They declared the last 10 yr of the current century the International Decade for Natural Disaster Reduction (IDNDR). Natural disasters are part of the environment in which we live. They adversely affect the lives of a large number of people and cause considerable damage to economy, nature, and property worldwide. Economic losses and losses of life from natural disasters are staggering. Moreover, they are much greater now than 30 yr ago. When fewer people lived on the earth, incidents of disasters were much less numerous, and humans were less vulnerable (Bruce 1994). Developing countries have much larger losses from disasters compared to the developed countries (United Nations Department of Humanitarian Aid 1993).

Nearly 85% of all natural disasters are directly related or associated with extreme weather events (Obasi 1994). Every day our planet experiences numerous extreme weather-induced disasters: droughts, floods, hurricanes, tropical cyclones, heat waves, tornadoes, bushfires, insect infestations, and many others. Among these, drought is the most damaging environmental phenomenon. The World Meteorological Organization of the United Nations estimated that in the quarter of a century since 1967, droughts have affected 50% of the 2.8 billion people who suffered

Corresponding author address: Mr. Felix N. Kogan, NOAA/NESDIS Room 712, NOAA Science Center, 5200 Auth Road, Camp Springs, MD 20746.
E-mail: fkogan@orbit.nesdis.noaa.gov
In final form 23 October 1996.

from weather-related disasters. Moreover, 1.3 million of the 3.5 million people killed by disasters between 1967 and 1991 were due to the direct and indirect cause of drought (Obasi 1994).

Only in the current decade have large-scale intensive droughts been observed on all continents. The most memorable droughts affected large areas in Europe, Africa, Australia, South, Central, and North America (Le Comte 1995, 1994). The impact of the most recent large-area severe drought (1988) on the U.S. economy has been estimated at $40 billion, which is 2–3 times the estimated losses from the 1989 San Francisco earthquake (Riebsame et al. 1990). The 1991–92 growing season in southern and eastern Africa was the worst since the beginning of the century when drought covered 2.6×10^6 mile^2 of the area and affected nearly 24 million people (United Nations Department of Humanitarian Aid 1993). Intensive drought occurred over large areas of Kazakhstan (part of the former Soviet Union) in 1991, devastating the environment and the agricultural economy. Grain production dropped nearly 40%. Unfortunately, the 1995 drought held the record and was more severe, lasted longer, and covered a much larger area than even the 1991 episode.

Timely information about the onset of drought, its extent, intensity, duration, and impacts can limit drought-related losses of life, minimize human suffering, and reduce damage to the economy and environment (Wilhite 1993). Weather data is a fairly good source of information that can be used for drought assessment. However, the sparsity of weather stations in some areas makes drought monitoring a daunting task. Lack of information about a drought becomes especially acute in areas where the weather station network is limited (e.g., sub-Saharan Africa). Furthermore, the data is often incomplete for the few available weather stations and/or not available early enough to enable timely drought detection and impact assessment. In addition, telecommunication problems, economic disturbances, and political and military conflicts also limit the availability of weather information.

Use of satellite data avoids most of these problems. Moreover, observations from space, especially from the National Oceanic and Atmospheric Administration (NOAA) operational polar-orbiting satellites, provide a unique vantage point, synoptic view, permanent data archive, extra visual information, cost effectiveness, and a regular, repetative view of nearly all of the earth's surfaces (Johnson et al. 1993). One of the most serious limitations of using Advanced Very High Resolution Radiometer (AVHRR) data for earth surface monitoring is considerable noise. However, the developed drought-monitoring algorithms consider the application of special processing tools in order to reduce this noise considerably.

Interest in using observations from operational satellites for developing numerical estimates of droughts and other environmental events has received enhanced attention over the last 10 yr as a substantial amount of satellite data obtained from the AVHRR has accumulated. The AVHRR-based reflectance in the visible (VIS) and near-infrared (NIR) wave bands and the Normalized Difference Vegetation Index [NDVI; NDVI = (NIR – VIS)/(NIR + VIS)] has been used in designing drought monitoring techniques (Kogan 1987).

Using multiyear observations, the NDVI was converted into the Vegetation Condition Index (VCI), which was applied successfully for drought monitoring and assessment of the vegetation condition in the United States (Kogan 1995a) and some other countries (Kogan 1994b). The Temperature Condition Index (TCI), developed recently from the AVHRR's thermal channels, increased the accuracy of drought monitoring, helped to explain the temperature contribution to the analysis of drought genesis, and also provided useful information for monitoring vegetation stress due to soil saturation (Kogan 1994a, 1995b). This paper describes the global application of the VCI–TCI indices for drought detection and monitoring, for the assessment of drought duration, area coverage, intensity, and impacts on vegetation. Considerable attention was devoted to collection and analysis of ground data to validate AVHRR-derived vegetation stress in different ecological environments and for various types of drought. The results presented in this paper show the high potential VCI–TCI indices have for maintaining a global drought watch.

2. General climatology of droughts

More than one-half of the terrestrial earth is susceptible to drought each year. Because drought is a recurring phenomenon and typical for the majority of world zones, the most productive lands of all continents can lose millions of tons of agricultural production annually. Social, physical, and economic impacts of drought can be staggering, especially in the developing countries. The immediate consequences of

drought include water-supply shortages, destruction of ecological resources, and losses of agricultural production, resulting in famine, human suffering, death, and abandonment of whole geographic regions.

The first impression of drought climatology can be obtained from the global distribution of the surface moisture balance. Figure 1 shows the climatological difference between annual precipitation and annual potential evaporation as an approximate measure of estimating vulnarability of territories toward drought (Gol'dsberg 1972).

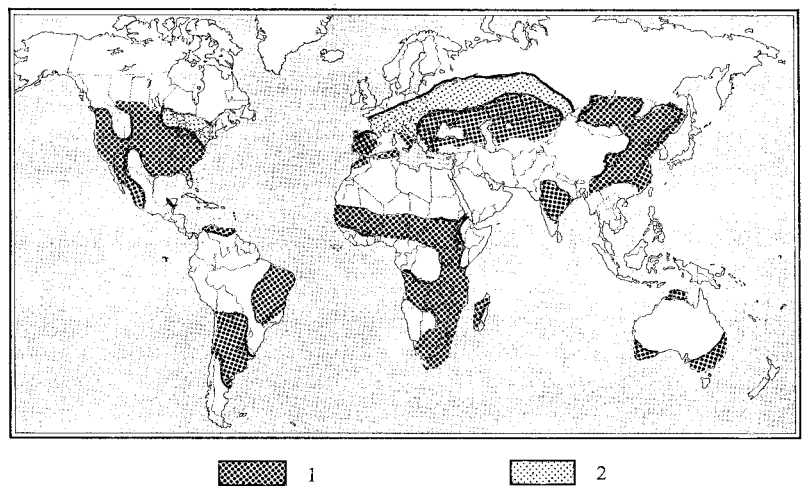

FIG. 1. Vulnerability of major agricultural areas to drought based on a difference between annual precipitation and potential evaporation (Gol'dsberg 1972); here, 1 indicates frequent intensive drought (difference −10 to −500 mm); and 2 indicates infrequent nonintensive drought (difference 0 to 200 mm).

The difference between annual precipitation and potential evaporation characterizes a balance between the moisture that an area receives in the form of precipitation and the amount of moisture that the available thermal resources of the same area are potentially able to evaporate. A positive or negative difference characterize correspondingly excessive or deficient moisture resources. In the areas with a negative balance, vegetation is likely to be potentially vulnerable to drought during the year. Although the farmers often compensate a lack of water irrigating crops, the resources of such water in agricultural areas are limited in general, especially in drought years and on a large area.

As seen in Fig. 1, even if the areas of hot deserts (water deficit above 800 mm) are disregarded, still there are large areas of the world that have a deficit of moisture. These are the areas of the biggest drought threat. The probability of droughts in these agricultural areas is above 25% but in semiarid zones can reach 75%–80% (Gol'dsberg 1972). It is important to emphasize, however, that large areas with a slightly positive difference (0–200 mm) have also up to 25% probability of drought occurrence (Gol'dsberg 1972). Only in the areas where precipitation exceeds potential evaporation by more than 200 mm are droughts extremely rare.

In summary, even if we discard nonagricultural areas—such as deserts, tropical forest, and mountains—and areas with a difference between annual precipitation and potential evaporation exceeding 200 mm, the remaining world area, which is sensitive to droughts, will amount to nearly 50%. More importantly, almost all major agricultural lands are located in this area. For example, as seen in Fig. 2 (Kogan 1986a), major wheat producing areas are in zones where annual potential evaporation is up to 400 mm higher than the amount of precipitation and are characterized by very frequent droughts (Gol'dsberg 1972). This supports the notion that "drought follows the plow" (Glantz 1994).

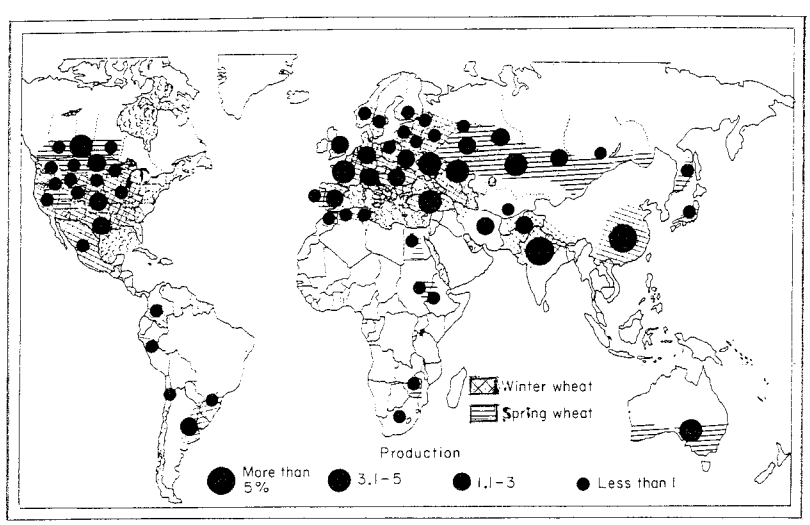

FIG. 2. Global distribution of wheat and production expressed as percentage of the total wheat production in 1980 (Kogan 1986a).

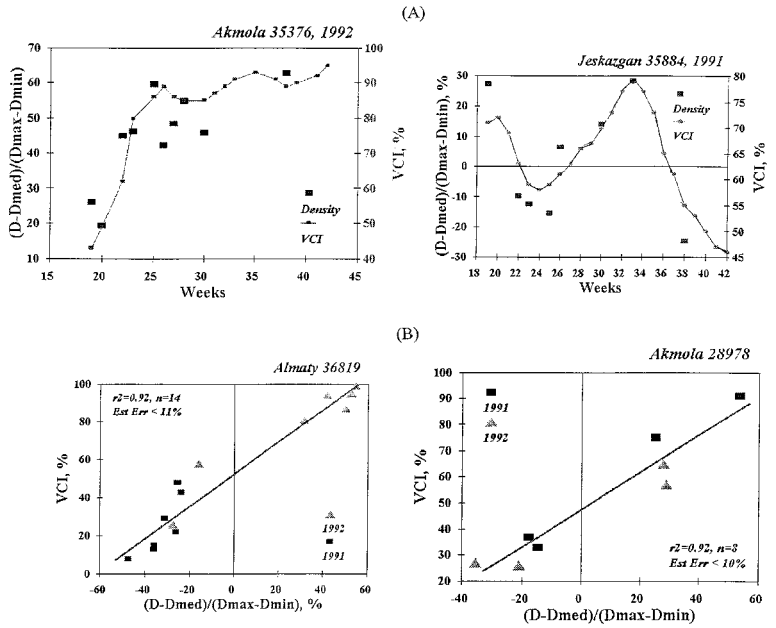

FIG. 3. Correlation between VCI and density of spring wheat at stations 35376 (49°53′N, 69°31′E), 35884 (46°02′N, 70°12′E), 36819 (44°08′N, 75°51′E), and 28978 (52°32′N, 68°45′E).

In the world's two largest agriculture-producing countries, the United States of America and the former Soviet Union (FSU), which produce nearly one-quarter of the total world grain, droughts occur almost every year. The heaviest damage to the economy and agriculture comes from large area intensive droughts. In the past century, the U.S. area affected by large-scale severe drought often exceeds 10% of the entire United States. Every 10–15 yr, the area exceeds 20% and, in some years, for example, the 1930s, reaches 65% of the entire country (Wilhite 1993).

Over the past 1000 yr of Russian history, catastrophic droughts occurred 8–12 times every century. Severe droughts are more frequent, especially in the areas with limited climatic and ecosystem resources. In Kazakhstan, where grain crops occupy nearly one-quarter of the total FSU grain area, around 35 severe and moderately large-area droughts occurred in the last 100 yr. In the Ukraine, where grain share accounts for nearly 20% of the total FSU grain production and where climate and soils are more favorable for growth than in Kazakhstan, droughts affect the area every 4–5 yr (Kogan 1986b).

3. Satellite and ground data

Satellite data were collected from the Global Vegetation Index (GVI) dataset (Kidwell 1994), which is one of the most widely used satellite products worldwide. The GVI is produced by sampling and mapping the 4-km daily radiance in the VIS (Ch1, 0.58–0.68 μm), NIR (Ch2, 0.72–1.1 μm), and two thermal bands (Ch4, 10.3–11.3 μm and Ch5, 11.5–12.5 μm) measured onboard NOAA polar-orbiting satellites, to a 16-km map. To minimize cloud effects, these maps, including the NDVI, solar zenith angle, and satellite scan angle, are composited over a 7-day period by saving those values that have the largest difference between VIS and NIR reflectance for each map cell. The weekly GVI data from April 1985 through November 1988 for *NOAA-9*, from December 1988 through September 1994 for *NOAA-11*, and during most of 1995 and 1996 for *NOAA-14* were used here.

During 1985–94, the performance of the VIS and NIR channels differed between *NOAA-9* and *NOAA-11* satellites and, most importantly, degraded over time for each satellite differently. Therefore, the standard data preparation procedure for the 7-day composite time series now includes a correction of VIS and NIR values following Rao and Chen (1995). The post-launch correction considerably improves the stability of NDVI over time, especially for *NOAA-9*, and almost eliminates the difference between the level of NDVI for the end of NOAA-9 and beginning of *NOAA-11* satellite data (Kogan et al. 1996). The thermal bands' measurements were converted to brightness temperatures using a look-up table, and a nonlinear correction was applied following Weinreb et al. (1990).

Recent advances in computer technology have stimulated the development of algorithms, the creation of global datasets and their wide distribution, and, most importantly, the development of products to characterize environmental parameters and phenomena (Kidwell 1994; Ohring et al. 1989; NOAA 1992; Los et al. 1994; Gutman et al. 1995; Goward et al. 1994; Maiden and Grego 1994; Kogan 1994b). Unfortunately, most of the products have not been validated against ground truth measurements. Therefore, in addition to collecting satellite data, a lot of effort was put in developing ground datasets in order to validate satellite-derived drought characteristics.

The ground data used in this study included rainfall; temperature; the Palmer Drought Index (PDI) and the Crop Moisture Index (CMI) data; and measurements of vegetation density, biomass, and yield. Monthly rainfall and temperature anomalies (deviation from the long-term means) for each first-order weather station were plotted on a map and areas of intensive weather anomalies were singled out. Vegetation density was measured by calculating the number of plants per unit area and expressed as a deviation from the multiyear median. Yield of agricultural crops and pastures is very sensitive to weather fluctuations and is reduced sharply in case of severe drought. This reduction can be used as an indicator of agricultural drought for validation of vegetation stress derived from the spectral vegetation indices. Therefore, average yield of grain crops for countries' administrative regions were used for validation of satellite-derived droughts.

4. Algorithm development

In the algorithm development, two crucial considerations were set forth: we avoided any aggregation of satellite data over space and/or time beyond the original resolution of GVI data. Space aggregation (average, interpolation) is inappropriate because areas with different environmental resources could be combined together. For example, an area of 1° lat $\times$ 1° long in the Sahel of Africa combine such different ecosystems as desert, grassland, and semiforest with differences between annual precipitation up to 1000 mm (Lebedev 1978). Temporal aggregation (biweekly, monthly) based on a compositing technique is biased because a later time interval is normally selected, giving preference to more developed vegetation. If the longer term average techniques is used, the results are quite often biased over space because neighboring pixels might characterize a different time interval (start and end of a month). Moreover, a 1-month time frame is too long to describe development of vegetation because morphological changes and leaf appearances occur every 3–7 days (Ulanova 1975). Weather patterns change even faster because an elementary synoptic period continues for 3–5 days. In case of severe drought, vegetation can be desicated in a matter of days. Therefore, drought monitoring on a monthly basis is inefficient. These considerations do not support more than 1 week's temporal aggregation of satellite data if they are to be used for monitoring vegetation and the related environmental phenomena.

The VCI and TCI were derived from the NDVI and Ch4 data, respectively, that were screened in order to eliminate high-frequency noise. Then NDVI and Ch4 data were stratified over space and time in order to describe land ecosystems and to enhance the weather-related component (Kogan 1990, 1995a; Kogan and Sullivan 1993). Noise in AVHRR data creates fundamental constraints to the remote sensing of earth surface. The sources of noise in NDVI data of the GVI product are summarized in Table 1 (Goward et al. 1991; Goward et al. 1993; Gutman 1991; Townshend 1994; Los et al. 1994; Justice and Townshend 1994). Clouds and other atmosphere constituents obscure the land surface, reducing NDVI considerably. In case of unusual events, such as a sharp increase in aerosols due to a volcanic eruption, NDVI can be depressed

TABLE 1. Source of noise in the Global Vegetation Index Dataset.

Clouds
Viewing Geometry
Bias toward off-nadir view
Surface anisotrophy
Atmospheric attenuation
Raleigh scattering
Aerosols
Water vapor
Mapping procedure
Off nadir view
9-day cycle
Changing footprint due to off-nadir view
Satellite orbital drift
Satellite change
Sensor degradation
Truncation
Daily sampling
Random noise
Represantativeness of sample
Human errors
Transmission
Adjustment of satellite parameters

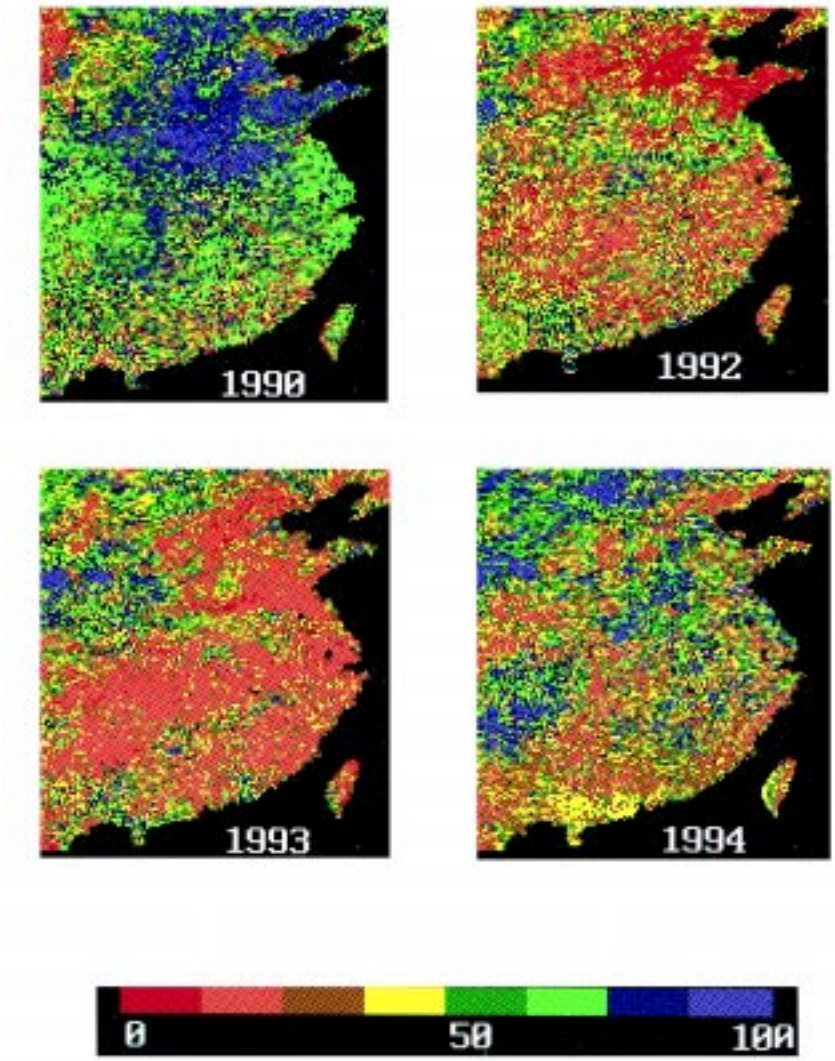

FIG. 4. End of July VCI/T4 in southeastern China.

for a long time (Kogan et al. 1994). Changes in viewing geometry can lead to both an increase and decrease in NDVI, depending on location, type of vegetation, and illumination. Satellite orbital drift, sensor degradation, and satellite change create long-term noise in NDVI data, especially after the satellite has been in service for more than 3 yr.

A few techniques have been designed to reduce some noise in AVHRR data. Several cloud-screening algorithms are presently available (Saunders and Kriebel 1988; Eck and Kalb 1991), although they have not been validated. Post-launch calibration correction (Rao and Chen 1995; Kidwell 1995) reduces the generally upward trend in NDVI time series. Thermal channels are corrected for the nonlinear behavior of the AVHRR sensor (Weinreb et al. 1990). Regardless of all these achievements, a complete physically based correction for all effects (Table 1) over various land surfaces, able to eliminate most of the high-frequency noise, is not available. Unfortunately, up to 90% of all NDVI and Ch4 annual time series values experience large fluctuations (Kogan 1995a), introducing some errors when these data are used for monitoring purposes. Up to 20% of these fluctuations are associated with nonphysical causes, such as method of data sampling and processing, satellite navigation and orientation, observation and communication errors, and other random noise. It is unlikely that corrections for this type of random noise will be developed. Furthermore, the present data improvement algorithms discard a pixel if any clouds are detected (Goward et al. 1994; Gutman et al. 1995). Since clouds usually cover a large area, the number of such pixels can be enormous over both space and time. Following Gutman (1991), nonconservative cloud screening discarded 60% of the pixels in the area with normal cloud climatology, leaving large areas without any land surface information. This put additional constraints on the use of AVHRR data.

Alternative techniques for high-frequency noise reduction in NDVI and brightness temperature (BT) data have been developed and widely used in the last 10 yr (van Dijk et al. 1987; Kogan et al. 1993). The vegetation-oriented techniques, which are used in this study to reduce noise considerably, stem from a statistical approximation of the vegetation and temperature dynamics during the annual cycle, complete suppression of high-frequency noise, and enhancement of low-frequency variations related to weather fluctuations. This technique considers smoothing the weekly time series with a combination of a compound median filter and the least squares technique (Kogan et al. 1993). This smoothing completely eliminated the high-frequency outliers, including random effects; approximated accurately the annual NDVI and BT cycles; and, more importantly, singled out low-frequency weather-related fluctuations (valleys and hills in the NDVI and

BT time series) during the annual cycle (Kogan 1995a).

After smoothing, interannual differences in NDVI and BT become more apparent. These differences are due to weather variation. For example, in dry years the NDVI curve will be lower and the BT curve will be higher than in normal and wet years. This principle of comparison of a dry year with other years in our archive was laid down in the next stage of the algorithm development. However, since the NDVI and BT quantify both spatial differences between productivity of ecosystems (ecosystem component) and year-to-year variations in each ecosystem due to weather fluctuations (weather component), and because the weather component values are much smaller than the ecosystem, the weather component needed to be separated from the ecosystem component (Kogan 1994a, 1995a).

This separation procedure consisted of stratification of the ecosystems, first, based on the 1985–93 minimum and maximum of NDVI and BT values for each pixel and week. The assumption was that maximum amount of vegetation is developed in years with optimal weather because such weather stimulates efficient use of ecosystem resources (e.g., increase in the rate of soil nutrition uptake). Conversely, minimum vegetation amount develops in years with extremely unfavorable weather (mostly dry and hot), which suppresses vegetation growth directly and also through a reduction in the rate of ecosystem resources use. For example, lack of water in drought years considerably reduces the amount of soil nutrient uptake. Therefore, the absolute maximum and minimum of NDVI and BT calculated from several years of data that contain the extreme weather events (drought and nondrought years) can be used as criteria for quantifying the extreme conditions (Kogan 1995a).

Following these considerations, the largest and the smallest NDVI and BT values during 1985–93 were calculated for each of the 52 weeks of the year and for each pixel. They were then used as the criteria for estimating the upper (favorable weather) and the lower (unfavorable weather) limits of the ecosystem resources. These limits characterize the "carrying capacity" of the ecosystems and the range in which NDVI and BT fluctuate due to weather changes from year to year in each ecosystem. These fluctuations were estimated relative to the maximum and minimum (max–min) intervals of both NDVI and BT variations and named the Vegetation (VCI) and Temperature (TCI) Condition Indices [Eqs. (1), (2), and (3)]. Since the NDVI and BT interpret oppositely extreme weather events (e.g., in case of drought, the NDVI is low and BT is high; conversely, in nondrought years, the NDVI is high while the BT is low), Eq. (2) was modified to reflect this opposite response of vegetation to temperature:

$$\mathrm{VCI} = 100(\mathrm{NDVI} - \mathrm{NDVI}_{\min})/(\mathrm{NDVI}_{\max} - \mathrm{NDVI}_{\min}), \quad (1)$$

$$\mathrm{TCI} = 100(T_{\max} - T)/(T_{\max} - T_{\min}), \quad (2)$$

where NDVI, $\mathrm{NDVI}_{\max}$, and $\mathrm{NDVI}_{\min}$ are the smoothed weekly NDVI, its multiyear absolute maximum, and minimum, respectively; and T, $T_{\max}$, and $T_{\min}$ are similar values for BT derived from Ch4 data. The VCI–TCI approximate the weather component in NDVI and BT values. They change from 0 to 100, reflecting changes in vegetation conditions from extremely bad to optimal. They were also combined in one index (VCI/T4) in order to express their additive approximation of vegetation stress:

$$\mathrm{VCI/T4} = (\mathrm{VCI} + \mathrm{TCI})/2. \quad (3)$$

With the development of the validation dataset, some weights will be assigned to the VCI–TCI indices.

5. Drought cases and validation

In recent years, the developed indices have been used successfully in detecting vegetation stress resulting from droughts in different part of the globe (Kogan 1994a, 1994b, 1995a, 1995b). The results of drought monitoring and validation in Asia, Africa, Europe, North and South America based on ground data are discussed below.

a. Asia

The following two examples feature Kazakhstan, part of the FSU, and China. Kazakhstan occupies nearly 1×10^6 mile^2, which is almost one-third of the size of the United States. The economy of Kazakhstan is highly dependent on agriculture, which has a grain and livestock orientation. Only one-tenth of Kazakhstan's land is sown to grain crops; the rest are rangelands, providing feed to large herds of sheep that graze all year around. A lack of rainfall and its high variability, frequent droughts, and desiccative winds are typical of Kazakhstan's climate, causing a two–three-fold variation in agricultural production.

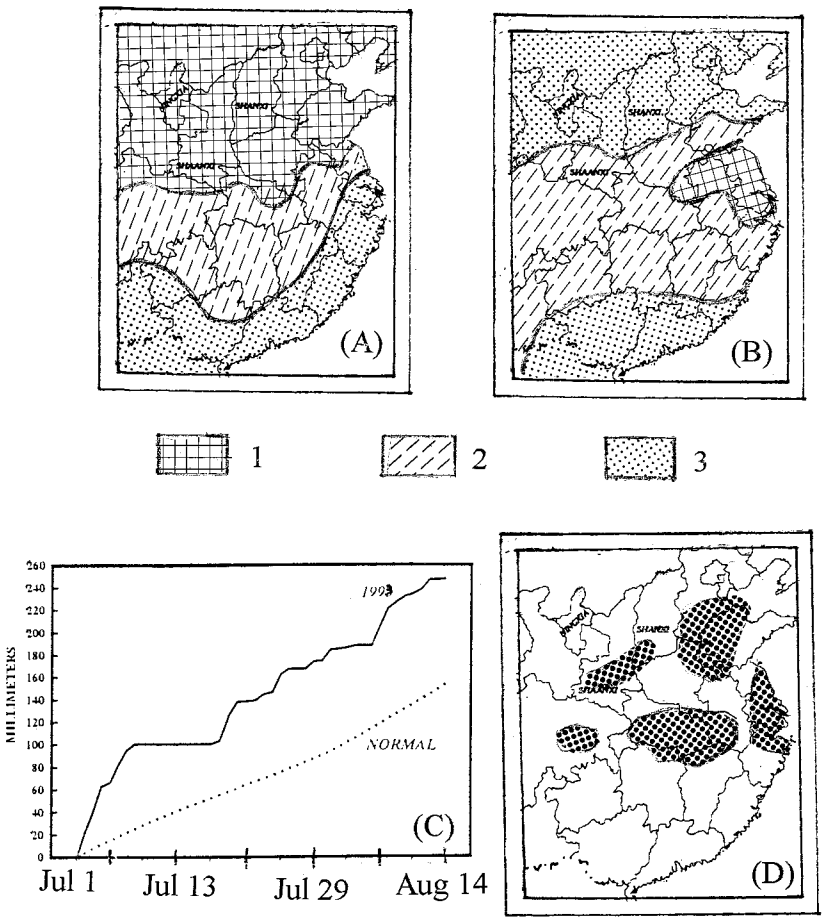

FIG. 5. Percent of normal precipitation (a) December 1993–May 1994 and (b) June–August 1994 (United States Department of Commerce 1994a–f); (c) 1993 cumulative daily rainfall, Hunan province (United States Department of Commerce 1993); (d) main cotton areas (United States Department of Agriculture 1994), southeastern China. For (a) and (b) rainfall, 1 is below normal, 2 is near normal, and 3 is above normal.

Recently, a cooperative effort (funded by the Agency for International Development of the United States) involving the Institute for Space Research, the National Meteorological Administration (Kazakhstan), the Desert Research Institute (Israel), and NOAA was directed toward development and validation of VCI-derived estimates of drought in Kazakhstan (Gitelson et al. 1996).

The 1991 and 1992 vegetation conditions were estimated from the VCI and the anomaly of vegetation density in Kazakhstan. Weekly VCI data were averaged for 3×3 pixel boxes around the area of field measurements. In an example from the main wheat area of northern Kazakhstan (Fig. 3), the VCI and density dynamics had close matching trends for both the dry (1991) and wet (1992) seasons. It is noticeable that, in both years, below normal density in early May (week 18) corresponded to the VCI-derived estimates of vegetation stress (VCI around 20). In early June, both indicators showed that the stress weakened in 1992 and intensified in 1991. At the end of June and in July (weeks 24–30), the conditions continued to improve in 1992 (density above mean and VCI above 50). They also improved in 1991, although both parameters were below 50. In the rangeland area of central (Akmola) and southern (Almaty) Kazakhstan, the VCI and density anomaly also showed strong correlation (Fig. 3b).

In 1994, China, which is the world leader in cotton production, unexpectedly purchased a large amount of cotton on the international market. The imports of cotton in 1994–95 exceeded by almost twofold the largest purchases since 1981. These purchases were preceded by a cotton yield reduction 3 yr in a row: 22% in 1992–93, 11% in 1993–94, and 7% in 1994–95 [the reduction was estimated relative to the average yield in a highly productive 1990–91 and 1991–92; United States Department of Agriculture (1994)]. The AVHRR data showed that the yield reduction can be attributed to vegetation stress in the main cotton-growing areas (Fig. 4). Of all 3 yr, 1992 had the most severe vegetation stress. Moreover, both VCI and TCI contributed to the stress that was typical for severe drought. These results were supported by below normal rainfall and above normal temperature during summer, particularly in July (United States Department of Commerce 1992).

Drought-related vegetation stress in the principal cotton-farming area was also observed in 1994 (Fig. 4). But the unusual weather feature of 1994 was the intensive preseason drought (Fig. 5a), which resulted in a deficient water supply for irrigated cotton. Fortunately, this deficit was partially offset by a near-normal summer rainfall (Fig. 5b). Therefore, the 1994 stress was much less intensive, over a smaller area, and resulted in an insignificant cotton yield reduction compared to 1992. Unlike 1992 and 1994, the 1993

AVHRR-derived vegetation stress in the cotton-growing area was estimated to be nondrought related because the values of the VCI were very low and those of the TCI very high. Weather data support this finding, showing a two-fold greater than normal rainfall during the critical period of cotton growth in July and August (Fig. 5c). Meanwhile, in 1993, vegetation was stressed over a larger area than in 1994, although the intensity of this stress was less than in 1992, consistent with cotton yield reduction.

b. Europe

The Ukraine (part of the FSU) is the largest country in southeastern Europe. Agriculture is one of the major sectors of the Ukrainian economy and it is very climate dependent. The most typical climatic feature limiting agricultural production is a deficit of precipitation, which increases toward the south and east. Water shortages are usually accompanied by hot and dry weather, and the usually light snow cover does not make up the summer moisture deficit. Droughts are very typical for the Ukrainian climate. They can occur anytime during the vegetation cycle but are most frequent in late spring and summer. Since 1872, droughts of various intensity occurred 57 times in the Ukraine (Selianinov 1958; Kogan 1986b). Catastrophic droughts happen in the area once every 60–80 yr. Moderate and severe droughts occur about 20% and 10% of the time, respectively. As a rule, droughts cover from 20% to 60% of the Ukrainian area and cause a 20%–50% decline in yield overall.

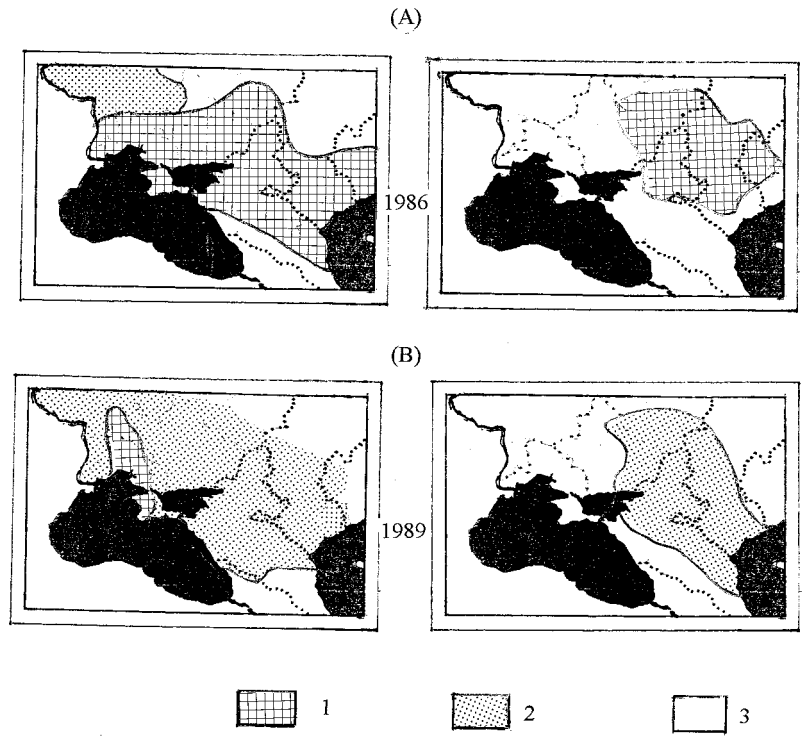

FIG. 6. (a) May–August precipitation anomaly and (b) grain yield departure from 10-yr mean, Ukraine; here, 1 is below normal, 2 is above normal, and 3 is no data.

In the past 10 yr, the Ukraine has had several large-area intensive droughts. One of them occurred in 1986, covering most of southern and eastern Ukraine and the adjacent regions to the east, and reduced agricultural production (United States Department of Agriculture 1994). Figures 6 and 7 compare the 1986 drought and the 1989 nondrought years. As seen, the 1986 late spring and summer rainfall was much below normal (in some areas less then 50%) during the 4-month period, specifically in the eastern part of the area (Fig. 6a), leading to a considerable reduction in grain yield (Fig. 6b). AVHRR data (Fig. 7) show very severe vegetation stress in the areas of rainfall deficit and yield reduction in 1986. In contrast to 1986, AVHRR-based estimates show mostly good conditions in 1989. These results were supported by an above normal rainfall and grain yield (Fig. 6b).

c. Africa

Across most of Africa, drought is a major natural disaster affecting nations' economies. Early drought detection, tracking, mapping, and severity assessment has been considerably constrained by incomplete meteorological data. Because of military and political conflicts and also economic deterioration in some of the regions, the rain gauge network density and the communications infrastructure have been steadily declining over the years, making drought detection and monitoring solely from rainfall data not always reliable. The AVHRR-based monitoring tool was tested in two countries, Zimbabwe in southern Africa and Ethiopia in east-central Africa. The agriculture of these countries is very important for food self-sufficiency, and food production is highly dependent on drought.

Droughts in Zimbabwe are associated with rainfall deficits depending mostly on the time of arrival and position of the intertropical convergence zone. In general, the climate of the northeast of the country is the wettest with 800 mm and the climate of the south is the

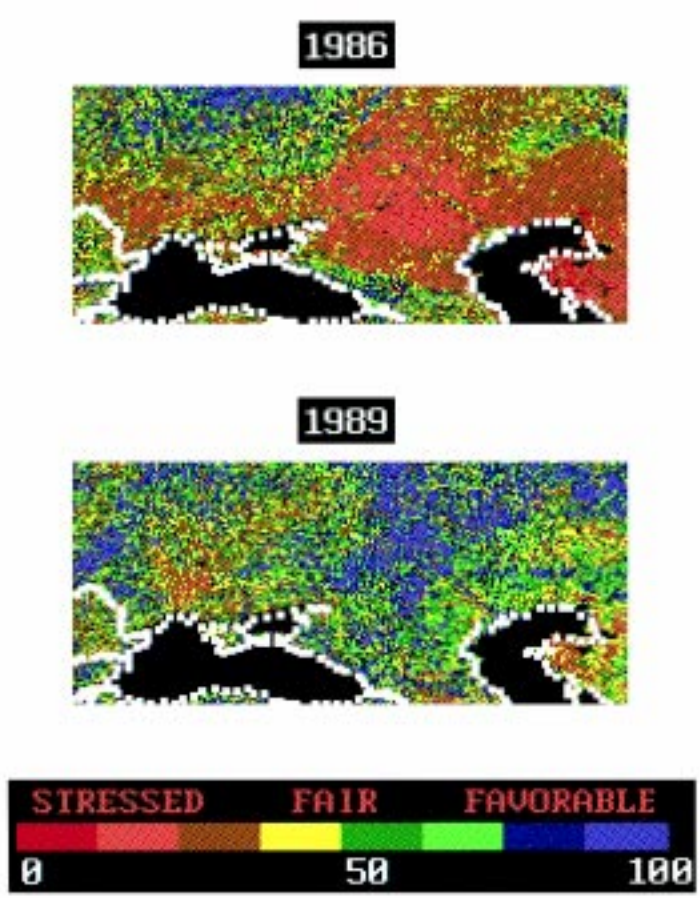

FIG. 7. End of July vegetation stress derived from VCI–TCI data, Ukraine.

driest with less than 400 mm annual rainfall. Maize is the most important food crop and is grown virtually everywhere. The northern provinces are considered to be a "bread basket," having the best soils and water supplies for intensive corn production (Kay 1976). Droughts can occur anywhere in the country, mostly during the growing season, causing significant crop failures. This is shown in Fig. 8 for one of the central provinces, which normally receives 630 mm of precipitation per year.

To test the spectral indices as a tool for drought monitoring, the weekly VCI–TCI values were averaged over each of the 54 administrative provinces of Zimbabwe and correlated with 9-yr corn yield anomalies (departure from the mean) during 1986–94.[1] Weather conditions in these years varied from favorable in 1988–89 to extremely unfavorable in 1991–92. As Fig. 9 shows, in most of the 54 provinces correlation between corn yield and weekly indices, when the weather is critical for crop growth, is very strong, 0.75–0.95. The correlation degrades in regions where corn area is small and/or environmental resources are very limited for successful farming. Thus, when crop yield is used as a validation tool in marginal areas, VCI–TCI spatial aggregation should be done only for the areas of intensive farming.

Moisture resources of Ethiopia are generally more favorable for agriculture than in Zimbabwe. Ethiopian climate provides an adequate amount of annual rainfall (500–1200 mm) in the areas of intensive farming, and numerous rivers have enough water for irrigation. The unusual feature of the Ethiopian environment that determines zoning is its rugged topography, which affects the distribution of rainfall, considerable runoff, and soil erosion. The main zones include a very dry pastoral one in the east, mixed farming area in the favorable plateau area (central), and high-altitude, extremely wet forest in the west. Although Ethiopia has a sufficient amount of rainfall, weather variability, especially dry and hot weather, is crucial and decisive in labor-intensive farming. Since the early 1970s, a series of very intensive droughts have affected Ethiopia, causing considerable damage to crops and the economy, which depends mostly on agriculture. The most memorable droughts, such as 1972, 1984, and 1991 (Yeshanew and Apparao 1989; Hellden and Eklundh 1981) resulted in the loss of natural resources, property, livestock, and thousands of human lives (Wodajo 1984; United Nations Department of Humanitarian Aid 1993).

An interesting case of dryness occurred during 1987 in Ethiopia. As reported by Yeshanew and Apparao (1989), that year is considered as extremely dry because precipitation for the entire country was the lowest since 1969, and eleven out of 14 administrative regions had more than a 10% deficit in rainfall during May–September (Figs. 10a,c). Contrary to

[1]This work was done with Mr. Unganai from the Drought Monitoring Center, Zimbabwe.

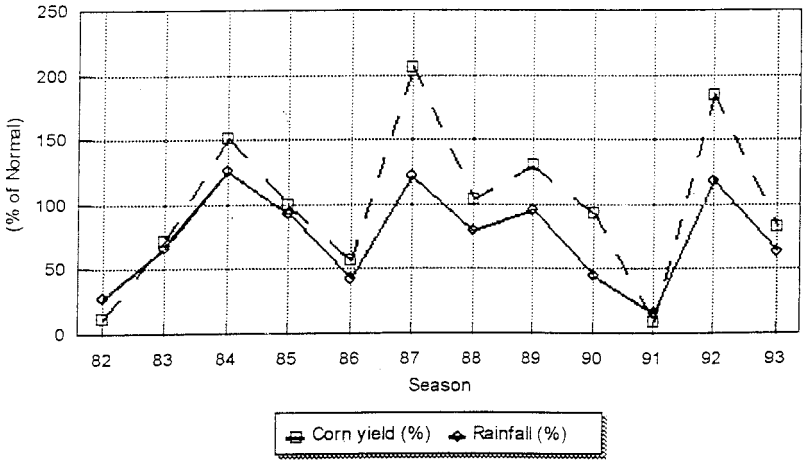

FIG. 8. Corn yield vs precipitation anomaly (departure from long-term mean) in Masvingo province, Zimbabwe.

the rainfall-derived intensive dryness (Fig. 10a), VCI/T4 data did not show significant vegetation stress. As seen in Fig. 11a, only slightly below normal vegetation conditions (VCI/T4 values 40–50) at the end of June 1987 were observed in southwestern Ethiopia, mostly due to temperature stress (see TCI4 image). Conditions in the southeastern pastoral zone were very favorable (VCI/T4, VCI, and TCI4 above 75), although severe rainfall deficits were reported there (Yeshanew and Apparao 1989). Only small areas in the farming zone of central Ethiopia indicated vegetation stress (VCI/T4 values 10–30) at the end of June 1987. However, the situation changed drastically by the end of August (Fig. 11b) when a large area of intensive vegetation stress appeared (both VCI and TCI4 below 30). This area coincided with the area of 19% reduction in corn yield (Fig. 10d). In other regions of Ethiopia, the yield anomaly was also in good agreement with VCI/T4 estimates of vegetation stress at the end of August: in the southeastern pastoral zone, corn yield was above normal and VCI/T4 estimated favorable conditions; in the western regions, mostly near-normal yield and conditions (around 50) were observed.

The discrepancies between weather and satellite data in interpreting the 1987 main season rainfall deficit in Ethiopia appeared because a very intensive meteorological drought (Yeshanew and Apparao 1989) did not turn into agricultural drought. This happened because abundant preseason (February–April) rainfall in 1987 (Fig. 10b) partially compensated for the precipitation deficit during the main season. Vegetation stress did not occur in the majority of regions and vegetation productivity was not reduced. This example emphasizes the value of the VCI/TCI tool for identifying agricultural drought.

d. North America

In 1988, the United States experienced unusually intensive, long, and extensive drought, which caused severe vegetation stress on about 25% of the total U.S. area. The most severe drought impacts were centered in the most productive agricultural land. This drought and its impacts have been evaluated based on both satellite and ground data (NOAA 1988; Riebsame et al. 1990; Kogan 1995a). However, one interesting case was discovered recently. In Iowa, which was in the epicenter of the 1988 drought, satellite data detected a large area where vegetation was stressed much less than in the neighboring areas (Fig. 12a). This case was investi-

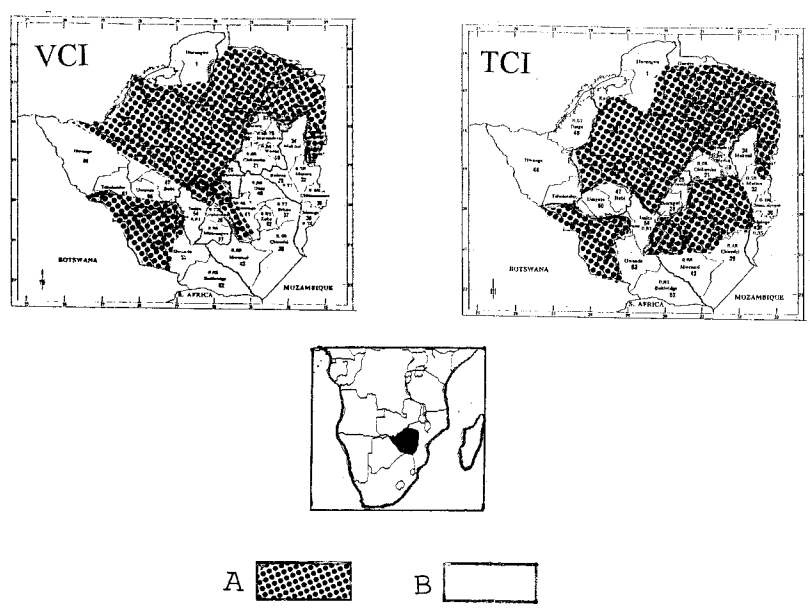

FIG. 9. Spatial distribution of correlation coefficients between corn yield departure from 9-yr mean and VCI–TCI for provinces of Zimbabwe, Africa: (a) 0.75–0.95; (b) 0.40–0.74.

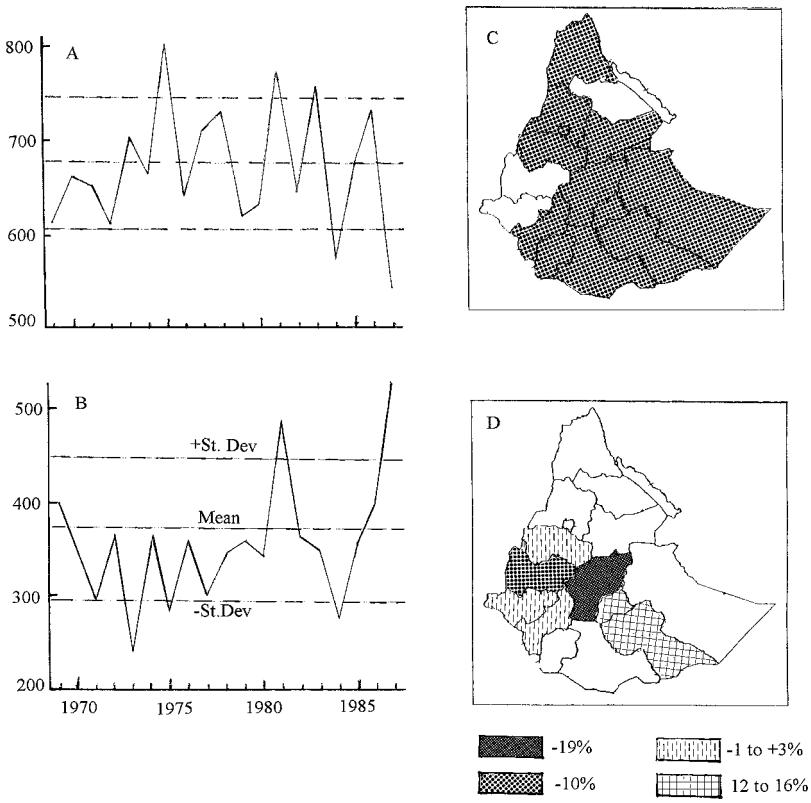

FIG. 10. Variability of the 1987 cumulative rainfall (mm) in Ethiopia during (a) May–September and (b) February–April. (c) Area with more than 10% rainfall deficit during May–September in administrative regions (after Yeshanew and Apparao 1989). (d) 1987 corn yield anomaly (departure from the 1979–83 mean yield).

gated with the Food and Agricultural Policy Research Institute of Columbia, Missouri, which provided corn yield data (A. Womack 1996, personal communication). Figure 12b shows the 1988 corn yield in each of Iowa's 99 counties, which belong to nine Crop Reporting Districts (CRD), in comparison with the average yield before and after the 1988 drought. Although Iowa's yield in 1988 was lower than in other years, it is seen that CRDs 1, 2, 4, and 7 had much higher average corn yield [20–30 bushels per acre (bu ac^{-1})] compared to CRDs 3, 5, 6, 8, and 9 (50–70 bu ac^{-1}). This twofold difference is explained by much more intensive vegetation stress in the southern and eastern third of Iowa, as the AVHRR data in Fig. 12a shows (VCI/T4 below 20). To our surprise, the PDI, which is used widely as a drought indicator, did not show the same pattern of drought/nondrought area and intensity (Fig. 12c) as the corn yield reduction and VCI/T4 data. The CMI was in a better agreement with yield and AVHRR data.

e. South America

Argentina is the second largest agricultural producer in South America. The complete agricultural crop statistics were collected for Cordoba, one of the main agricultural provinces in Argentina, to test the drought monitoring tool.[2] The weekly VCI–TCI were calculated for 26 departments of the Cordoba area (as a mean value for the area) and compared with the average for each province's crop yield anomaly (departure from the 9-yr mean) from 1985–86 to 1993–94. The analysis was done for corn, which is the major crop in central and eastern Cordoba. Corn yield anomalies were correlated with weekly VCI–TCI starting from the first week in July (winter in Southern Hemisphere) and ending with the last week in June of the next calendar year

[2]This work was done in cooperation with Dr. R. Seilers, professor at the University of Rio Cuarto, and my colleague Dr. J. Sullivan.

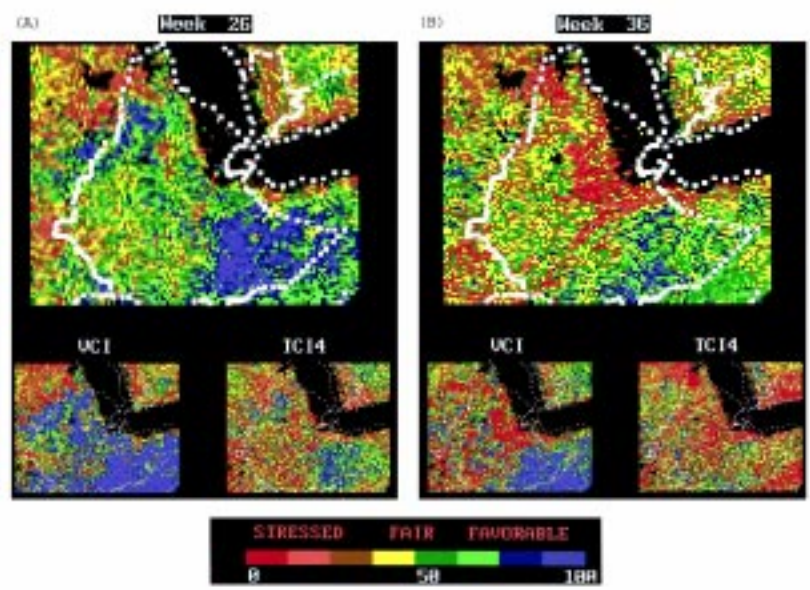

FIG. 11. Assessment of vegetation condition based on VCI/T4, VCI, and TCI4 at the end of June (week 26) and at the end of August (week 36) 1987.

(total 52 weeks). Two main crop growing departments, Juarez Celmon (34% of Cordoba total crop area) and Rio Cuarto (nearly 10%) were selected for analysis. Corn is the principal crop in these departments, occupying 90% and 50% correspondingly, of the area under main crops.

Figure 13 shows a strong and positive correlation between corn yield anomaly and VCI–TCI, indicating an increase in yield anomaly for the higher VCI–TCI. This relationship is the strongest during the critical period of corn growth (January–February), and the correlation coefficient is slightly larger for VCI than for TCI, for example, in Rio Cuarto, 0.92 versus 0.85. In addition, the time of the highest VCI correlation occurs 2–3 weeks earlier than for TCI, mid-January versus early February, correspondingly. Also, the VCI and TCI value of around 60 is a breaking point, identifying corn yield to be above or below multiyear mean. If both VCI and TCI are below 35–40 for a few weeks, more than 50% of corn yield reduction can be expected. The correlation analysis over time can be used to outline the critical period during the growing season where VCI and TCI have the highest information about corn yield fluctuation. For example, in Rio Cuarto, this period covers December through February.

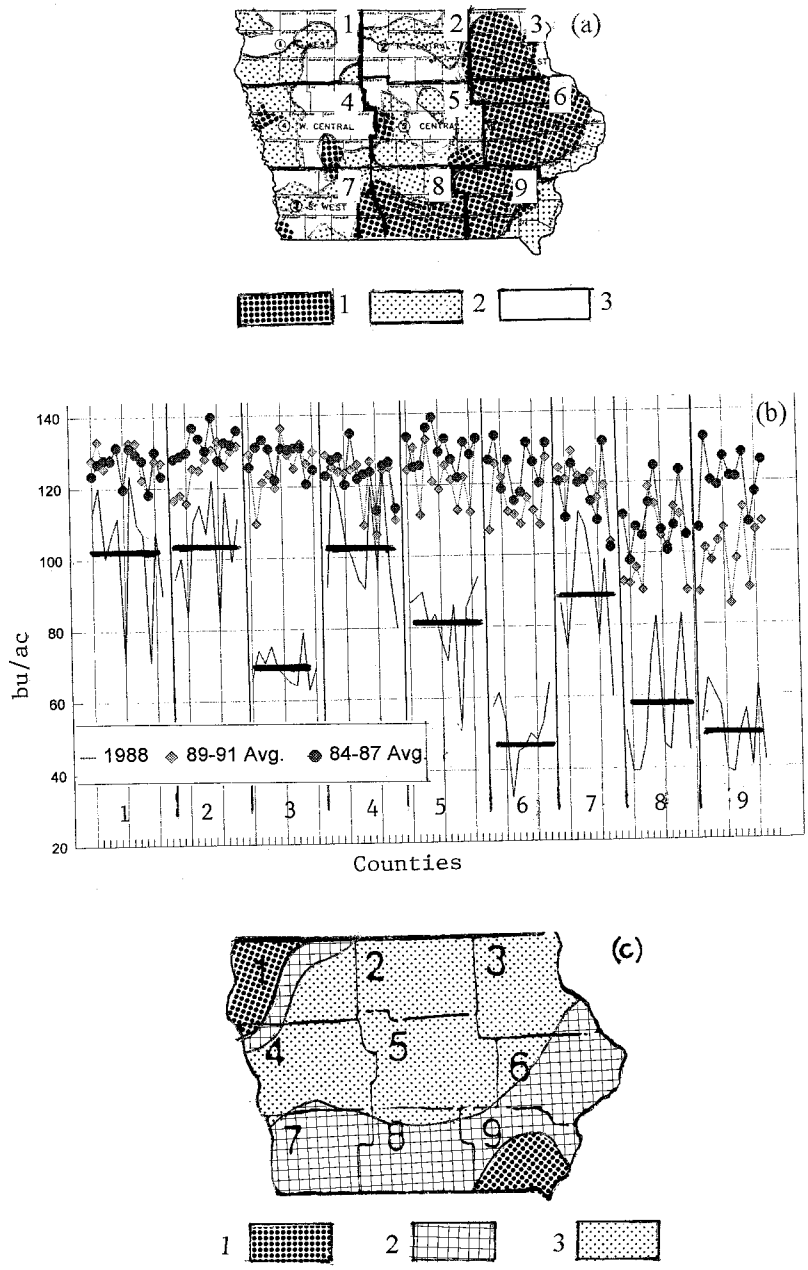

FIG. 12. VCI/T4-based vegetation condition at the end of June 1988 in Iowa. (a) Here, 1 represents stressed, 2 represents fair, and 3 represents favorable. (b) County mean corn yield (bushels per acre); counties grouped in 1–9 CRDs. (c) PDI at the beginning of July 1988 (United States Department of Commerce 1988); here, 1 is severely dry, 2 is excessively dry, and 3 is abnormally dry.

6. Conclusions

The validation results clearly indicate the utility of VCI–TCI as a sole source of information about vegetation stress and consequently drought as a major cause of the stress. Moreover, they were also useful for real-time assessments and diagnosis of vegetation condition and weather impact on vegetation. This information is especially beneficial if weather data is not available and/or nonrepresentative due to sparsity of a weather-observing network. If real-time weather information is reliable, it should be combined with the AVHRR-derived characteristics and used as a comprehensive tool for monitoring vegetation stress, drought estimates, and weather impact assessment.

Since February 1995, the AVHRR sensor on the newly launched *NOAA-14* operational polar-orbiting satellite has provided information about vegetation stress. After some adjustments made to Ch1, Ch2, and

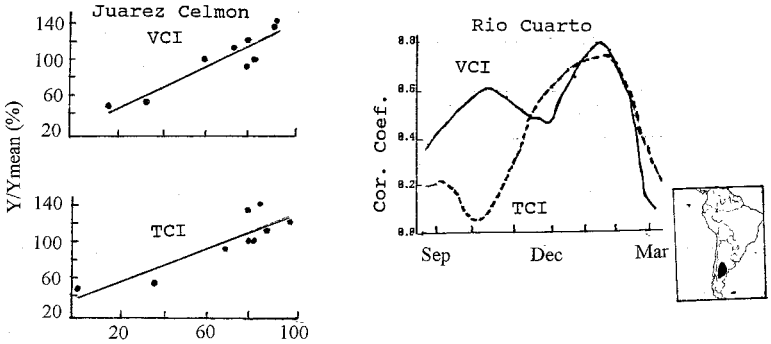

FIG. 13. Correlation of corn yield (departure from mean) with VCI and TCI in two departments of Cordoba province, Argentina.

Acknowledgments. The author thanks his colleague Dr. J. Ellis for extremely useful discussions, comments, and generous suggestions; Dr. Sullivan for contributions with software development and very useful discussions; and Dr. J. Tarpley for his support and suggestions. Special appreciation should be given to the author's collaborators Dr. A. Gitelson, professor at Ben-Gurion University of the Negev, Israel; Dr. A. Womack, professor at the University of Missouri-Columbia; Dr. R. Seilers, professor at the University of Rio Cuarto, Argentina; Mr. L. Unganai from the Drought Monitoring Center, Zimbabwe; and Dr. L. Spivak from the Space Research Institute, Kazakhstan, for contributing their data and valuable time.

Ch4 in order to correct for post-launch degradation and also for the application of the algorithms discussed, we continued to use VCI–TCI for vegetation monitoring, particularly for the analysis of drought-related stress. Preliminary results indicated that the VCI/T4 index identified areas of the world that experienced drought in 1995, for example, the drought in Kazakhstan discussed in this paper.

In 1996, VCI–TCI data indicated early season severe vegetation stress on the Great Plains of the United States. Preliminary data analysis showed (Fig. 14) that the 1996 stress at the end of April surpassed the 1988 dry spell in the heart of the winter wheat growing areas of Kansas, Oklahoma, Missouri, and Texas. However, in 1989, the vegetation stress was resulted from a much more intensive, long dryness, especially in central and eastern Kansas and northern and southern Texas. In contrast, most of Oklahoma was severely affected by the 1996 drought. These results were validated by in situ data and this analysis will be continued using new ground-truth data and new areas.

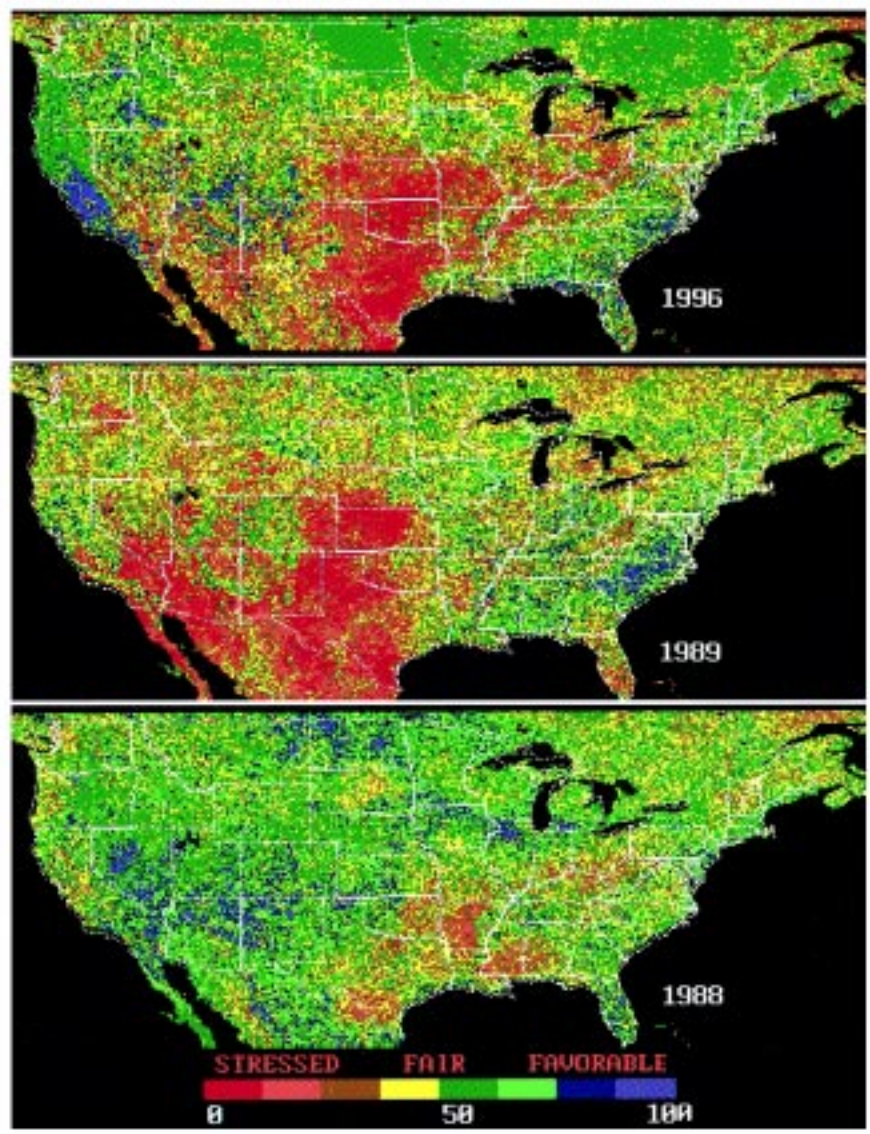

FIG. 14. VCI/T4-derived droughts of 1996, 1989, and 1988 at the end of April (week 16) in the winter wheat area of the United States.

References

Bruce, J. P., 1994: Natural disaster reduction and global change. *Bull. Amer. Meteor. Soc.,* **75,** 1831–1835.

Eck, T. F., and V. L. Kalb, 1991: Cloud screening for Africa using geographically and seasonally variable infrared thresholds. *Int. J. Remote Sens.,* **12,** 1205–1221.

Gitelson, A., F. Kogan, E. Zakarin, L. Spivak, and L. Lebed, 1996: Estimation of seasonal dynamics of pasture and crop productivity in Kazakhstan using NOAA/AVHRR Data. *Proc. IGARSS '96: Remote Sensing for a Sustainable Future,* Lincoln, NE, 209–211.

Glantz, M. H., 1994: Drought, desertification, and food production. *Drought Follows the Plow,* M. H. Glantz, Ed., Cambridge University Press, 9–30.

Gol'dsberg, I., Ed., 1972: *Agroclimatic Atlas of the World.* Hydrometizdat, 133 pp.

Goward, S. N., B. Markham, D. G. Dye, W. Dulaney, and J. Yang, 1991: Normalized difference vegetation index measurements from the Advanced Very High Resolution Radiometer. *Remote Sens. Environ.,* **35,** 257–277.

——, D. G. Dye, S. Turner, and J. Yang, 1993: Objective assessment of the NOAA Global Vegetation Index data product. *Int. J. Remote Sens.,* **14,** 3365–3394.

——, S. Turner, D. G. Dye, and S. Liang, 1994: The University of Maryland improved global vegetation index product. *Int. J. Remote Sens.,* **15,** 3365–3397.

Gutman, G. G., 1991: Vegetation indices from AVHRR data: An update and future prospects. *Remote Sens. Environ.,* **35,** 121–136.

Gutman, G., D. Tarpley, A. Ignatov, and S. Olson, 1995: The enhanced NOAA global land data set from the Advanced Very High Resolution Radiometer. *Bull. Amer. Meteor. Soc.,* **76,** 1141–1156.

Hellden, U., and L. Eklundh, 1988: *National Drought Impact Monitoring—A NOAA NDVI and Precipitation Data Study of Ethiopia.* Lund University Press, 55 pp.

Johnson, G. E., V. R. Achutuni, S. Thiruvengadachari, and F. Kogan, 1993: The role of NOAA satellite data in drought early warning and monitoring. *Drought Assessment, Management, and Planning: Theory and Case Studies,* D. A. Wilhite, Ed., Kluwer Academic, 31–49.

Justice, C. O., and J. R. G. Townshend, 1994: Data sets for global remote sensing: Lessons learnt. *Int. J. Remote Sens.,* **15,** 3621–3639.

Kay, G., 1976: Rhodesia. *World Atlas of Agriculture: Africa.* Vol. 4. Istituto Geografico De Agostini–NOVARA, 449–460.

Kidwell, K. B., Ed., 1994: Global vegetation index user's guide. U.S. Department of Commerce Tech. Rep., 51 pp.

——, Ed., 1995: NOAA polar orbiting data user's guide. U.S. Department of Commerce Tech. Rep.

Kogan, F. N., 1986a: Climate constraints and trends in global grain production. *J. Agric. Forest Meteor.,* **37,** 89–107.

——, 1986b: The impact of climate and technology on Soviet grain production. Delphic Association Rep., 174 pp.

——, 1987: Vegetation index for areal analysis of crop conditions. Preprints, *Proc. 18th Conf. on Agricultural and Forest Meteorology,* West Lafayette, IN, Amer. Meteor. Soc., 103–107.

——, 1990: Remote sensing of weather impacts on vegetation in non-homogeneous areas. *Int. J. Remote Sens.,* **11,** 1405–1419.

——, 1994a: Application of vegetation index and brightness temperature for drought detection. *Adv. Space Res.,* **15**(11), 91–100.

——, 1994b: NOAA plays leadership role in developing satellite technology for drought watch. *Earth Observation Mag.,* September, 18–21.

——, 1995a: Droughts of the late 1980s in the United States as derived from NOAA polar orbiting satellite data. *Bull. Amer. Meteor. Soc.,* **76,** 655–668.

——, 1995b: AVHRR data for detection and analysis of vegetation stress. *1995 Meteorological Satellite Data Users' Conference,* Winchester, United Kingdom, EUMETSAT, 155–162.

——, and J. Sullivan, 1993: Development of global drought-watch system using NOAA/AVHRR data. *Adv. Space Res.,* **13**(5), 219–222.

——, J. Sullivan, R. Carry, and J. Tarpley, 1994: Post-Pinatubo vegetation index in central Africa. *Geocarto Int.,* **9**(3), 63–66.

——, J. T. Sullivan, and P. B. Ciren, 1996: Testing post-launch calibration for the AVHRR sensor on world desert targets during 1985–1993. *Adv. Space Res.,* **17**(1), 47–50.

Lebedev, A. N., Ed., 1978: *Climatic Atlas of Africa* (in Russian). Part 2. Hydrometizdat, 166 pp.

Le Comte, D., 1994: Weather highlights around the world. *Weatherwise,* **47,** 23–26.

——, 1995: Weather highlights around the world. *Weatherwise,* **48,** 20–22.

Los, S. O., C. O. Justice, and C. J. Tucker, 1994: A global 1 by 1 degree NDVI data set for climate studies derived from GIMMS continental NDVI data. *Int. J. Remote Sens.,* **15,** 3493–3518.

Maiden, M. E., and S. Grego, 1994: NASA's pathfinder data set program: Land surface parameters. *Int. J. Remote Sens.,* **15,** 3333–3345.

NOAA, 1988: Drought advisory 88/12: Summary of drought conditions and impacts. NOAA, September 29, 8 pp.

——, 1992: Global Change Data Base. Digital Data with Documentation. NOAA/NGDC.

Obasi, G. O. P., 1994: WMO's Role in the international decade for natural disaster reduction. *Bull. Amer. Meteor. Soc.,* **75,** 1655–1661.

Ohring, G., K. Gallo, A. Gruber, W. Planet, L. Stowe, and D. Tarpley, 1989: Climate and global change: Characteristics of NOAA satellite data. *Eos, Trans. Amer. Geophys. Union,* **70,** 41.

Rao, C. R. N., and J. Chen, 1995: Inter-satellite calibration linkages for the visible and near-infrared channels of the Advanced Very High Resolution Radiometer on the NOAA-7, -9, and -11 spacecrafts. *Int. J. Remote Sens.,* **16,** 1931–1942.

Riebsame, W. E., S. A. Changnon, and T. R. Karl, 1990: *Drought and Natural Resource Management in the United States: Impacts and Implications of the 1987–1989 Drought.* Westview Press, 174 pp.

Saunders, R. U., and K. T. Kriebel, 1988: An improved method for detecting clear sky and cloudy radiances from AVHRR data. *Int. J. Remote Sens.,* **9,** 123–150.

Selianinov, G. T., 1958: Origin and dynamics of droughts. *Droughts in the USSR, Their Origin, Probability, and Impact on Yield* (in Russian), A. Rudenko, Ed., Hydrometizdat, 5–31.

Townshend, J. R. G., 1994: Global data sets for land applications from the Advanced Very High Resolution Radiometer: An introduction. *Int. J. Remote Sens.*, **15,** 3319–3332.

Ulanova, E. S., 1975: *Climate and Winter Wheat Yield*. Hydrometizdat, 298 pp.

United Nations Department of Humanitarian Affairs, 1993: *DHA News,* May/June, 6–10, 26–27.

United States Department of Agriculture, 1994: Major world crop areas and climatic profiles. Agricultural Handbook No. 664, 279 pp.

United States Department of Commerce, 1988: Weekly weather and crop bulletin. Vol. 75, No. 28, 12 July, 4 pp.

——, 1992: Weekly weather and crop bulletin. Vol. 79, No. 37, 15 September, 29 pp.

——, 1993: Weekly weather and crop bulletin. Vol. 80, No. 33, 17 August, 23 pp.

——, 1994a: Weekly weather and crop bulletin. Vol. 81, February 15.

——, 1994b: Weekly weather and crop bulletin. Vol. 81, March 22.

——, 1994c: Weekly weather and crop bulletin. Vol. 81, April 19.

——, 1994d: Weekly weather and crop bulletin. Vol. 81, May 17.

——, 1994e: Weekly weather and crop bulletin. Vol. 81, June 21.

——, 1994f: Weekly weather and crop bulletin. Vol. 81, July 19.

van Dijk, A., S. L. Callis, C. M. Sakamoto, and W. L. Decker, 1987: Smoothing vegetation index profiles: An alternative method for reducing radiometric disturbance in NOAA/AVHRR data. *Photogr. Engin. Remote Sens.*, **53,** 1059–1067.

Weinreb, M. P., G. Hamilton, and S. Brown, 1990: Nonlinearity correction in calibration of the Advanced Very High Resolution Radiometer infrared channels. *J. Geophys. Res.*, **95,** 7381–7388.

Wilhite, D. A., 1993: The enigma of drought. *Drought Assessment, Management, and Planning: Theory and Case Studies*, D. A. Wilhite, Ed., Kluwer Academic, 3–15.

Wodajo, T., 1984: Agrometeorological activities in ethiopia. Prospects for improving agroclimatic/crop condition assessment. Final Rep.

Yeshanew, A., and G. Apparao, 1989: Annual rainfall potential and its variability in drought years over Ethiopia. *Conf. on Climate and Water,* Helsinki, Finland, Academy of Finland, 219–235.